Journal of Electroceramics, 7, 121–126, 2001
© 2002 Kluwer Academic Publishers. Manufactured in The Netherlands.

Structural, Electrical and Dielectric Behavior of $Pb(Mg_{1/4}Ni_{1/4}W_{1/2})O_3$ Ceramics

SHASHI K. SINHA,[1] S.N. CHOUDHARY[1] & R.N.P. CHOUDHARY[2]
[1]*University Department of Physics, T.M. Bhagalpur University, Bhagalpur 812007, India*
[2]*Department of Physics and Meteorology, Indian Institute of Technology, Kharagpur 721302, India*

Submitted August 4, 2000; Revised February 1, 2001; Accepted August 16, 2001

Abstract. Polycrystalline samples of $Pb(Mg_{1/4}Ni_{1/4}W_{1/2})O_3$ (PMNW) have been prepared by a conventional solid-state reaction. Preliminary room temperature X-ray study shows the formation of single-phase compound with cell parameters $a = 9.8045$ (28) Å, $b = 13.1280$ (28) Å and $c = 14.42072$ (28) Å. Dielectric anomaly and ferroelectric phase transition observed at 76°C was supported by our polarization study. The variation of dc resistivity of the material with temperature shows its semiconducting behaviour.

Keywords: dielectrics, phase transition, orthorhombic, dc resistivity, polarization

1. Introduction

With the growing interest and suitability for device applications, a large number of ferroelectric ceramics have been developed in a wide variety of compositions and stable structures. Oxide ferroelectrics synthesized by single crystal, thin film and ceramics routes are now widely used in computer memory, electro-optical modulators, pyroelectric and gas sensors, transducers, hydrophones and others electronics devices [1–8]. The Pb-based perovskite compounds such as $PbTiO_3$, $Pb(ZrTi)O_3$, $Pb(MgNb)O_3$ etc. are important for wide ranging applications [9–13]. The PMNW compound belongs to the perovskite ABO_3(A = mono, divalent ions, B = tri-hexavalent ions) family, with some modifications/substitutions at the B-site. Extensive literature survey on Pb-based complex perovskite shows that, except a few studies, not much work has been reported on complex $PbWO_3$ and $PbMoO_3$ because of their high electrical conductivity and dielectric loss at low frequency and at high temperature. Recently a diffuse phase transition has also been observed in many complex tungstate/molybdate [14–17] ceramics modified with alkali and rare-earth ions. This attracted us to make other complex compounds modified with other isovalent ions such as Mn^{2+}/Mg^{2+} and/or Cd^{2+}, Zn^{2+}, Ni^{2+}, Cu^{2+} etc. at W- or Mo-sites. We here report preliminary structural and detailed dielectric, polarization reversal and resistive properties of $Pb(Mg_{1/4}Ni_{1/4}W_{1/2})O_3$ (here after PMNW) for a better understanding of its phase transition and dielectric behavior.

From an extensive literature survey it is found that except for a few works, not much is known about other members of this family. Therefore we have attempted to study the existence of the ferroelectric–paraelectric phase transitions in the compounds of a general formula $Pb(B'_{1/4}B''_{1/4}B'''_{1/2})O_3$ where B′ = alkaline earth ions, B″ = transition ions and B‴ = tungsten or molybdenum ions. In the present communication, we report preliminary structural and microstructural and detailed dielectric and electrical properties of $Pb(Mg_{1/4}Ni_{1/4}W_{1/2})O_3$ (hereafter PMNW) compounds.

2. Experimental Details

Polycrystalline samples of PMNW were prepared by a high-temperature (∼860°C) solid-state reaction technique using high purity component oxides and carbonate: PbO (99.99% M/s Aldrich chemical company, Inc. USA), NiO (Black) (90%, M/s Loba Chemie, India), WO_3 (AR grade B.D.H. Chemical Ltd., UK)

and $MgCO_3$ (99% M/s s.d. Fine Chemicals Pvt. Ltd., India) in a desired stoichiometry. These oxides and carbonate were thoroughly mixed in an agate mortar for 2 h and calcined at 760°C for 12 h in an alumina crucible in an air atmosphere. The mixing and calcination were repeated at 820°C for 18 h. Finally, the calcined powder of PMNW was used to make cylindrical pellets of diameter 10 mm and thickness 1–2 mm under an isostatic pressure of about 6.5×10^7 N/m^2. Polyvinyl alcohol (PVA) was used as binder to reduce the brittleness of the pellets. The binder was burnt out during the sintering process. The pellets were sintered in an alumina crucible at 860°C in an air atmosphere for 8 h.

Room temperature (298 K) X-ray diffraction (XRD) pattern of calcined powder was recorded using a Philips X-ray powder diffractometer (PW1710) with Cu K_α radiation ($\lambda = 1.5418$ Å) in a wide range of Bragg angles ($15^\circ \leq 2\theta < 80^\circ$) with a scanning rate of 2°/min. The surface morphology of the different portions of the sample was examined with the help of CAMSCAN-180 scanning electric microscope (SEM) with different magnifications. The sintered pellet sample was grounded and lapped to make the surface flat and parallel, and subsequently electroded with silver paste to both flat surfaces.

The dielectric constant (ε) and loss ($\tan\delta$) of the yellowish and hard pellet sample were obtained as a function of frequency (400 to 10^4 Hz) at room temperature and as a function of temperature (30–300°C) at a fixed frequency of 10 kHz over a small temperature interval using a GR 1620 AP capacitance measuring assembly in conjunction with a laboratory-made three-terminal sample holder to compensate stray capacitance. The temperatures were recorded using a chromel-alumel thermocouple.

The dc volume resistivity of the pellet sample was measured as a function of temperature (30–380°C) at a constant electric field of 60 V/cm using a Keithley-617 programmable electrometer. The temperature variation of the polarization and the coercive field of the samples were recorded at 50 Hz with an ac field of 8.5 kV/cm using a dual-trace oscilloscope connected to a modified Sawyer–Tower circuit [18].

3. Results and Discussion

The sharp and single X-ray diffraction (XRD) peaks of PMNW quite different in position and intensity from the diffraction peaks of all other component oxides/carbonate suggested the formation of a single-phase new compound. All the peaks of the XRD pattern were indexed and unit cell parameters were determined in various crystal systems using a standard computer program "PowdMult". Finally, an unit cell in orthorhombic system was selected for which the sum of differences in observed and calculated d-values i.e. $\sum \Delta d = \sum (d_{\text{obs}} - d_{\text{cal}})$ was found to be a minimum. Table 1 shows the good agreement between observed and calculated d-values, which suggests the correctness of the selection of the crystal system and cell parameters. The orthorhombic unit cell parameters, refined by least-squares methods are $a = 9.8045$ (28) Å: $b = 13.1780$ (28) Å and $c = 14.4207$ (28) Å. It was not possible to determine the space group of the compound with a limited number of reflections. The scattered linear particle size (P_{hkl}) was calculated from strong and medium intensity peaks using Scherrer's Eq. [19]. $P_{hkl} = 0.89\,\lambda/\beta_{1/2}\,\text{Cos}\,\theta_{hkl}$ where $\beta_{1/2}$ = half peak of reflection). The average value of P_{hkl} was found to be 185 Å, which is comparable to that determined from particle size analysis and SEM. SEM micrograph (Fig. 1) shows that grains are uniformly distributed in space and size on the surface of the sintered sample. The grains are nearly spherical and their average size is 173 Å.

Figure 2 shows the variation of ε and $\tan\delta$ as a function of frequency (200–10^4 Hz) at room temperature. The nature of variation of these parameters shows that ε and $\tan\delta$ decrease with the increase of frequency which is an expected behavior of a dielectric. The high value of ε at low frequency is due to the presence of all types of polarisations (viz. electronic, dipolar, interfacial, orientational etc.) in the compound at room temperature. As the frequency was increased some of these polarisations were ineffective, and hence at higher frequency we had a lower value of ε. The $\tan\delta$ was found to vary in a similar way as ε.

Figure 3 shows the variation of ε and $\tan\delta$ as a function of temperature at 10 kHz. The dielectric constant ε increases rapidly to its maximum value $\varepsilon_{\max} = 147$ around 76°C. Above 76°C it decreases to a value of 135 at 225°C. Above 225°C it increases vary rapidly. This rapid increase of dielectric constant is due to space charge polarization in the compound. A pressed sample develops a considerable amount of space charge polarization arising from defects in the bulk and/or at the surface of the material contributing to an increase in ε value and loss particularly at low frequencies and high temperature. The lattice defect concentration

Table 1. Comparison of some observed and calculated d-values (in Å) of some reflections for PMNW compound at room temperature.

h	k	l	d_{obs}	d_{cal}	I/I_0
1	0	2	4.6417	4.6472	16.42
1	2	0	4.5964	4.6053	22.76
0	3	2	3.9896	3.9917	5.64
0	4	1	3.4722	3.4717	4.47
0	2	4	3.2374	3.2535	7.3
0	4	2	3.2094	3.2106	5.23
1	0	4	3.1401	3.1238	4.65
1	4	0	3.0796	3.0734	2.89
0	7	3	3.0091	2.9972	2.07
1	8	0	2.9007	2.8970	4.47
1	8	1	2.8230	2.8294	100
1	0	4	2.7307	2.7332	1.82
1	3	4	2.6260	2.6282	1.49
1	5	4	2.4636	2.4681	0.84
2	0	1	2.4104	2.4110	6.39
0	6	5	2.3079	2.3072	25.55
0	10	4	2.1650	2.1641	0.96
0	4	6	2.0981	2.0986	1.82
2	6	2	2.0708	2.0718	0.76
1	1	6	1.9988	1.9982	29.19
0	7	6	1.9345	1.9350	1.54
0	1	3	1.8345	1.8344	3.04
0	5	7	1.7873	1.7875	1.88
0	14	4	1.7407	1.7410	0.58
1	4	7	1.7076	1.7059	0.88
3	1	0	1.6323	1.6324	33.58
2	13	1	1.6274	1.6289	16.42
1	3	8	1.5403	1.5400	3.35
2	16	2	1.4140	1.4147	14.70
1	19	2	1.4104	1.4110	7.06
2	9	7	1.3520	1.3520	2.07
2	6	8	1.3127	1.3141	0.72
3	6	6	1.2645	1.2645	7.18
3	13	4	1.2204	1.2206	0.96

increases with temperature making the space charge polarization more dominant and ε increases with temperature [10, 20]. Space charge polarization typically occur at low frequencies $<10^3$ Hz and may be associated with ion migration and electrode contact losses or with the presence of grain boundary or inhomogeneous phases in the dielectric. Space charge polarization losses in the latter case can occur up to much higher frequencies $\sim 10^5$ Hz [21]. Here migrating charge carrier cations and anions in the material causing the space charge polarization collect near the cathodes and anodes respectively. This distorts the electric field and increases the capacitance of the material. It is clear from Fig. 3 that PMNW underwent a phase transition at 76°C. The dielectric loss also varies in a similar way. However, the peak is broadened around the maximum ε, which indicates the existence of diffuse phase transition. The reason for diffuseness of the dielectric peak was examined by an empirical formula [17]. $1/\varepsilon - 1/\varepsilon_{max} = C(T - T_c)^{\gamma}$ or, $\ln[1/\varepsilon - 1/\varepsilon_{max}] = \ln C + \gamma \ln(T - T_c)$ where ε is the dielectric constant at temperature T and ε_{max} is its maximum value at T_c. The value of exponent γ is a measure

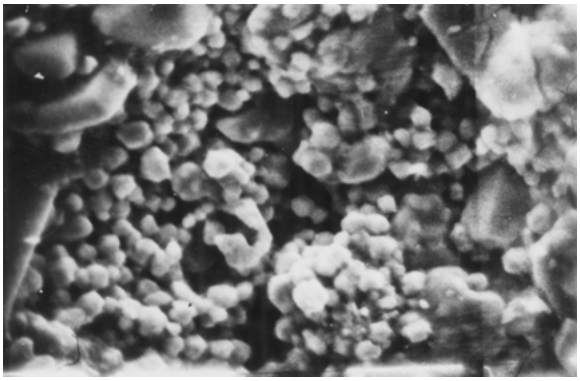

Fig. 1. SEM micrograph of PMNW at 10 μm magnification.

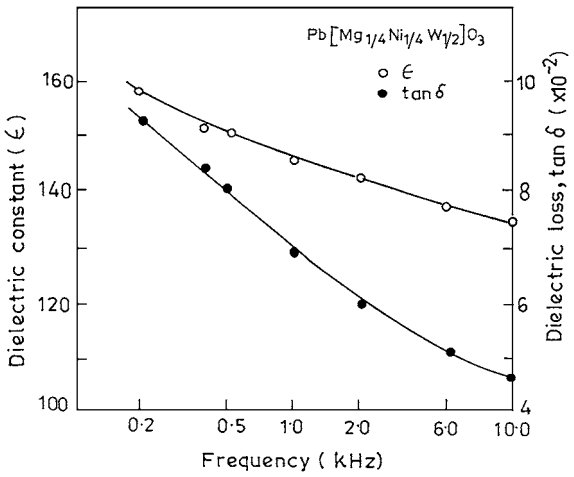

Fig. 2. Variation of dielectric constant (ε) and loss ($\tan\delta$) of PMNW with frequency at room temperature.

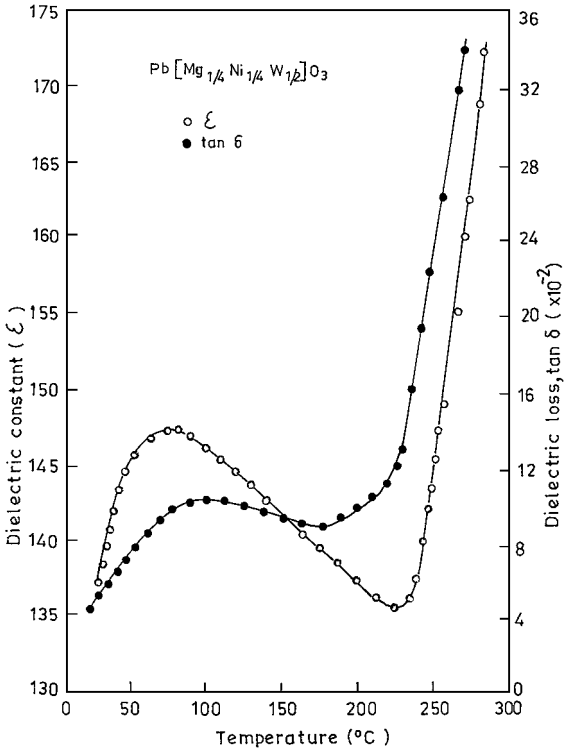

Fig. 3. Variation of dielectric constant (ε) and loss ($\tan\delta$) of PMNW as a function of temperature at 10 kHz.

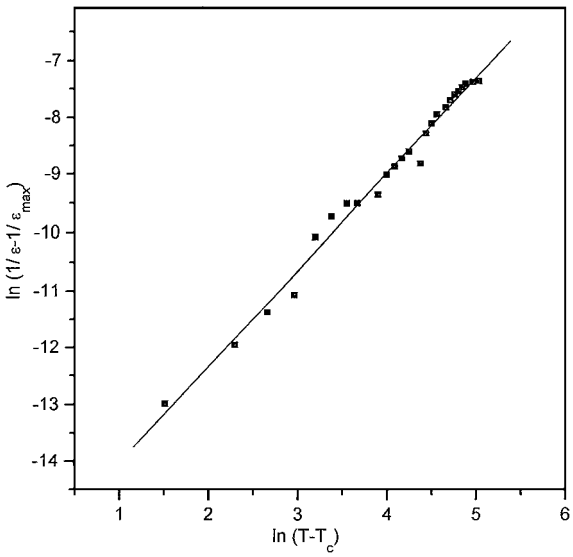

Fig. 4. Variation of $\ln(1/\varepsilon - 1/\varepsilon_{\max})$ of PMNW with $\ln(T - T_c)$.

of the degree of disorderness. The value of γ, measured from the slopes of $\ln[1/\varepsilon - 1/\varepsilon_{\max}]$ vs. $\ln(T - T_c)$ plot (Fig. 4) was found to be 1.76. This suggests that compound does not show pure Curie–Weiss type behavior during any temperature variational study and has the characteristics of a diffuse phase transition. This diffuseness is due to the compositional fluctuation and structural disordering in the arrangement of cations in one or more crystallographic sites of the structure [22, 23]. This suggests a microscopic heterogeneity in the compound with different local Curie points. Such behavior has also been found in modified lead niobates/tungstate compounds [24–26].

The ac electrical conductivity σ_{ac} and activation energy of the material were calculated from the dielectric data collected at different temperature using the standard formula $\sigma = \omega\varepsilon_o\varepsilon \tan\delta$ and $\sigma = \sigma_o \exp(-E_a/k_BT)$ respectively. Here ε_o = vacuum dielectric constant, ω = angular frequency and k_B = Boltzmann constant. In the present investigation these parameters have been used to represent the observed experimental data. The a.c. conductivity (σ_{ac}) is caused by the losses due to bound charges or the charges hoping between the well-defined sites, without contributing anything to long range motion or dc conductivity (σ_{dc}). But every material have some free or delocalized charges, which give rise to dc conductivity without contributing anything to dielectric polarization. It is assumed that ac and dc conductivity is due to completely different processes or where the same basic process is responsible for both types of conductivity. But the states giving rise to the ac conductivity are clustered and do not constitute a percolation path throughout the sample (and hence do not contribute to the dc conductivity) suggesting that if the same process is responsible for both dc and ac conductivity, σ_{dc} is simply the $\omega \to 0$ limit of $\sigma_{ac}(\omega)$ and the validity of the equation for total conductivity $\sigma_t(\omega) = \sigma_{dc} + \sigma_{ac}(\omega)$ will be dubious. The value of activation energy E_a obtained (for 10 kHz dielectric data) from the slope of the curve ln σ_{ac} vs. $1/T$ (Fig. 5) was 0.82 eV.

The temperature dependence of dc conductivity of PMNW at a constant biasing field of 61 V/cm is shown in Fig. 6. It is observed that dc conductivity increases with increasing temperature. Due to addition of thermal energy the electrons could be set free from O^{2-} ions. When an electron is introduced in the sample it might be associated with cations and hence results in an unstable valence state [21]. This type of resistive behavior is found in many ferroelectric materials studied by us [24–26]. Moreover Maass et al. [27] also

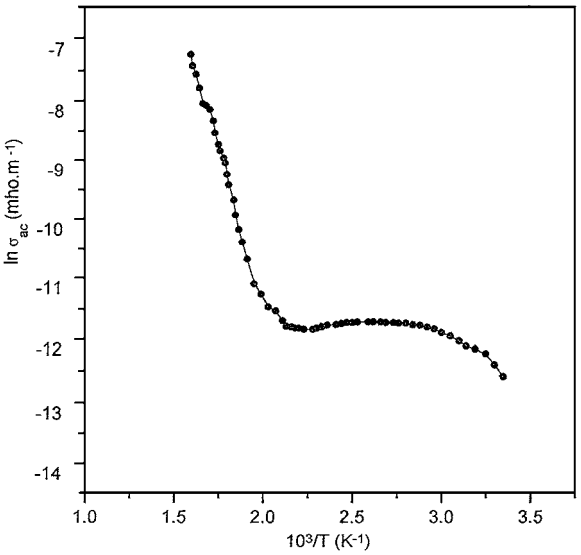

Fig. 5. Variation of ac conductivity ($\ln \sigma_{ac}$) of PMNW as a function of inverse of absolute temperature ($10^3/T$).

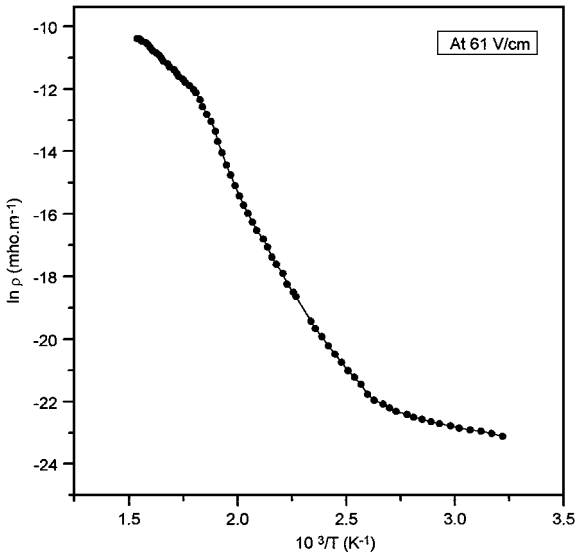

Fig. 6. Variation of dc conductivity ($\ln \sigma_{dc}$) of PMNW as a function of temperature at a constant electric field (61 V/cm).

pointed that local environment of any cation is largely unaffected by the addition or presence of cations. As a matter of fact the mobile ions create and maintain their own distinctive and preferred environment and do not *make do* with the sites left over by dissimilar cations (Pb^{2+}, Mg^{2+}, Ni^{2+}, and W^{6+}). Cations in oxide ferroelectrics have also indicated to involve creation and maintenance of favorable oxygen environment around

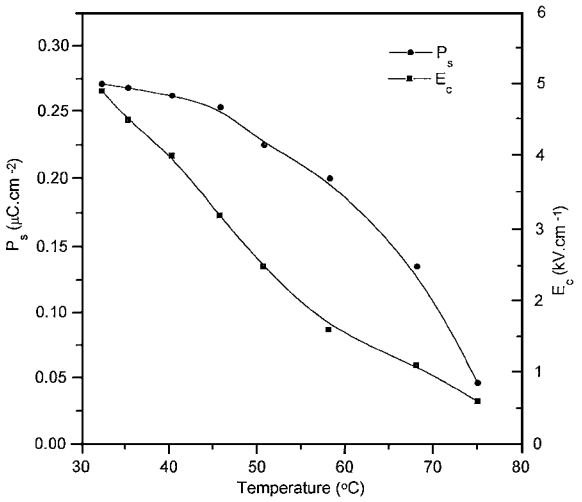

Fig. 7. Variation of spontaneous polarization (P_s) and coercive field (E_c) as a function of temperature at 50 Hz.

them. The activation energy obtained from the slope of the $\ln \sigma_{dc}$ vs. $1/T$ was found to be 0.96 eV. The high value of activation energy in the high temperature region clearly indicates that some ionization has taken place inside the sample at high temperature.

The variation of spontaneous polarization and coercive field is shown in Fig. 7. As the ceramic sample has lower density than that of a single crystal, a higher electric field is required to obtain saturation polarization. On the other hand, at higher field the sample breaks into small pieces. Therefore, we have optimized a field (8.5 kV/cm) to observe the loop. The spontaneous polarization and coercive field were determined from the hysteresis loop. As the material was lossy and sufficient field could not be applied because of the dielectric breakdown, we could not get a proper hysteresis loop. However the spontaneous polarization and coercive field were found decreasing with increasing temperature until it becomes zero or very small. Both experimental evidences of the dielectric anomaly and the polarization measurements confirmed the phase transition. For the ceramic sample a constant spontaneous polarization was observed above T_c. This can be explained by the nature of domains present in the ceramics. The ceramic sample has a large number of domains having a different direction of polarization in spite of a single polar axis as it has in a single crystal. Due to application of external ac electric field, the dipoles in each and every domain experience a force to oscillate about their mean position of rest. When thermal energy

is supplied to it, the dipole may agitate and rearrange randomly. But some of them still have a definite dipole moment, which results in a small value of spontaneous polarization above T_c.

Figure 7 shows that coercive field is approximately a linear function of temperature where as spontaneous polarization appears to be quadratic. These relationships confirm that a second order phase transition occurs in PMNW materials.

Finally it is concluded that PMNW has orthorhombic structure at room temperature and undergoes ferroelectric phase transition at 76°C.

Acknowledgments

The authors are thankful to Dr. T.P. Sinha, Bose Institute, Calcutta for his some experimental help.

References

1. L.H. Parker and A.F. Tasch, *IEEE Cir. and Dev. Mag*., **6**, 17 (1990).
2. T. Hawaguchi, H. Adachi, K. Setsune, O. Yamazaki, and K. Wasa, *Appl. Optics*, **23**, 2187 (1984).
3. K.K. Deb, *Ferroelectrics*, **82**, 45 (1988).
4. L.A. Thomas, *Ferroelectrics*, **3**, 231 (1972).
5. R.P. Tandon, R. Singh, R.D.P. Singh, and S. Chandra, *Ferroelectrics*, **120**, 293 (1991).
6. R.P. Tandon, R. Singh, V. Singh, N.H. Swami, and V.K. Hans, *J. Mater. Sci. Letters*, **11**, 882 (1992).
7. Z. Surowiak and D. Czekaj, *Thin Solid Films*, **214**, 78 (1992).
8. T. Ikeda and T. Okana, Japan. *J. Appl. Phys*., **3**, 63 (1964).
9. K.L. Yadav, R.N.P. Choudhary, and T.K. Chaki, *J. Mater. Sci*., **27**, 5244 (1991).
10. S. Sharma, R.N.P. Choudhary, and R. Sati, *J. Mater. Sci. Letters*, **12**, 530 (1993).
11. S.R. Shantigrahi, R.N.P. Choudhary, and H.N. Acharya, *Mater. Sci. Engg. B*, **60**, 31 (1999).
12. S.R. Shantigrahi, R.N.P. Choudhary, H.N. Acharya, and T.P. Sinha, *J. Appl. Phys*., **85**(3), 1713 (1999).
13. S.R. Shantigrahi, R.N.P. Choudhary, H.N. Acharya, and T.P. Sinha, *J. Phys. D Appl. Phys*., **32**, 1539 (1999).
14. S. Bera and R.N.P. Choudhary, *J. Phys. Chem. Solids*, **60**, 767 (1999).
15. S. Bera and R.N.P. Choudhary, *Mat. Letters*, **37**, 111 (1998).
16. S. Bera and R.N.P. Choudhary, *Mat. Letters*, **46**, 154 (2000).
17. S.M. Pilgrim, A.E. Sutherland, and S.R. Winzer, *J. Am. Ceram. Soc*., **73**, 3122 (1990).
18. J.K. Sinha, *J. Sci. Instrum*., **42**, 696 (1965).
19. P. Scherrer, *Cottinger Nachrich*., **2**, 98 (1918).
20. S. Sharma, R.N.P. Choudhary, and R. Sati, *J. Mater. Sci. Letters*, **13**, 1151 (1994).
21. R.C. Buchanan, *Ceramic Materials for Electronics* (Marcel Dekker Inc., New York, 1986).
22. L.E. Cross, *Ferroelectrics*, **76**, 241 (1987).
23. C. Schmidt, *Ferroelectrics*, **78**, 199 (1988).
24. S. Sharma, R. Sati, R.N.P. Choudhary, and T.P. Sinha, *Mat. Letters*, **16**, 281 (1993).
25. S. Sharma, R. Sati, and R.N.P. Choudhary, *Phy. Stat. Solidi*., **133a**, 491 (1992).
26. S. Bera and R.N.P. Choudhary, *Mat. Letters*, **22**, 197 (1995).
27. P. Maass, A. Bunde, and M.D. Ingram, *Phys. Rev. Letters*, **68**, 3064 (1992).